mater.scichina.com link.springer.com

Published online 14 June 2023 | https://doi.org/10.1007/s40843-022-2466-7
Sci China Mater 2023, 66(8): 3337–3346

Water-retaining and separable adhesive hydrogel dressing for wound healing without secondary damage

Zhuangzhuang Zhang[1,2], Yajie Zhang[2*], Yuanshan Liu[1,2], Penghui Zheng[2], Tong Gao[2], Bingqing Luo[1,2], Xingzhu Liu[2], Fanshu Ma[2], Jine Wang[1,2*] and Renjun Pei[1,2*]

ABSTRACT As a type of wound dressings, adhesive hydrogel dressings have been studied widely. However, due to the problems of moisture loss and secondary damage during dressing changes, the clinical application of adhesive hydrogel dressing remains a significant challenge. Herein, we developed a water-retaining and separable adhesive hydrogel wound dressing composed of methacrylated silk fibroin (SFMA), tannic acid (TA), and urethane diacrylate (UDA). The addition of TA with an abundance of catechol groups endowed the hydrogel with improved mechanical properties, good tissue adhesion and hemostasis abilities. Then, a hydrophobic polyurethane diacrylate (PUA) coating encapsulated the hydrogel by UDA polymerization, which could maintain the long-lasting high water content of the hydrogel. Furthermore, due to the adhesion energy being higher than the fracture energy of the hydrogel, it could be separated upon peeling. Finally, the animal experiments indicated that this adhesive hemostatic hydrogel could increase wound healing efficiency by maintaining long-lasting moist environment and being changed without secondary damage. These results showed that the multifunctional hydrogel might be a promising wound dressing for clinical application.

Keywords: adhesive hydrogel, water retention, separability, no secondary damage, wound dressing

INTRODUCTION

Skin is a multilayer organ that covers the surface of the human body and has the functions of defending the body against bacteria attacks, preventing body dehydration, and feeling external temperature [1,2]. However, skin is susceptible to injury from multiple factors such as cullet and knives [3]. Once the skin suffers an injury, it often needs wound dressing to achieve rapid closure and accelerate wound healing [4]. Due to the low cost and good hemostatic properties, gauze is the most commonly used wound dressing [5,6]. Unfortunately, gauze often causes severe secondary damage to the injured wound during gauze changes because the newly grown tissue is adhered tightly by gauze [4,7,8]. In addition, studies have shown that a moist healing environment facilitates the migration and proliferation of endothelial cells, fibroblasts, and epithelial cells, whereas traditional gauzes provide a dry healing environment, which is not favorable for wound healing [9–11].

Due to the advantages of high water content, biophysical similarity to natural tissue, and good tissue adhesion, adhesive hydrogels as wound dressings have aroused the interest of many researchers [12,13]. Adhesive hydrogels can not only adhere to the wound to close it and stop bleeding, but also act as a physical barrier to isolate the external environment and provide a moist environment to accelerate wound healing [14,15]. Tannic acid (TA), a natural polyphenol extracted from various plants, has valuable properties such as antibacterial and anti-inflammation abilities [16–18]. Importantly, TA can react with many polymers by hydrogen bonding because of its availability of catechol groups [19,20]. Since TA-based hydrogels with good adhesion ability can be obtained simply by mixing TA and polymers, such hydrogels are widely used in wound healing [18,20,21]. Nevertheless, almost all TA-based adhesive hydrogels typically dehydrate and shrink when exposed to open air, leading to the loss of flexibility and the moist environment, as well as causing unnecessary secondary damage to the newly formed tissue during dressing changes, which extremely limits their clinical applications [22,23].

Much research shows that the addition of highly hydrated salts or excess organic solvents can effectively improve the water retention properties of hydrogels, but these methods usually result in high osmotic pressure and poor biocompatibility [24–26]. Currently, a new strategy to improve the water retention capacity of hydrogel is to encapsulate the hydrogel with a hydrophobic coating [27–29]. Especially, the hydrophobic polyurethane diacrylate (PUA) coating polymerized from urethane diacrylate (UDA) using an "inside-out" technology can encapsulate a wide variety of hydrogels with various types and shapes easily, thus, preventing the evaporation of water from the hydrogel [27]. But this strategy has not yet been used in hydrogel wound dressings. We hypothesize that good water-retaining ability can also be obtained with adhesive hydrogels by encapsulating surfaces that do not contact to the wound with the PUA coating.

Recently, the method of on-demand removal has often been used to decrease secondary damage [4,30,31]. For example, Jiang *et al.* [30] developed a skin-friendly and painless removable adhesive hydrogel patch composed of polymerized gallic acid and gelatin methacryloyl (GelMA). The patch could adhere tightly to the warm skin and be removed on-demand through

[1] School of Nano-Tech and Nano-Bionics, University of Science and Technology of China, Hefei 230026, China
[2] CAS Key Laboratory for Nano-Bio Interface, Division of Nanobiomedicine, Suzhou Institute of Nano-Tech and Nano-Bionics, Chinese Academy of Sciences, Suzhou 215123, China
[*] Corresponding authors (emails: rjpei2011@sinano.ac.cn (Pei R); yjzhang2016@sinano.ac.cn (Zhang Y); jewang2012@sinano.ac.cn (Wang J))

the shrinkage of the thermoresponsive GelMA chain after placing an ice bag above the patch. Based on the pH-sensitive coordination bond (catechol-Fe) and dynamic Schiff base bonds, Liang *et al.* [31] developed an adhesive hydrogel with on-demand removal or dissolution after the intervention of deferoxamine mesylate (DFO) solution. Generally, the on-demand removal of adhesive hydrogels was triggered by additional factors, which is inconvenient in practical application. In this study, we designed an adhesive hydrogel, whose adhesion energy was higher than its fracture energy, allowing it to be separated into parts upon peeling, and causing little wound damage during dressing changes, which has barely been reported.

In this work, a PUA-coated methacrylated silk fibroin/TA (SFMA/TA (ST)) hydrogel wound dressing with good tissue adhesion, long-lasting water retention, and separable abilities was prepared (Fig. 1). Firstly, SF was modified with glycidyl methacrylate (GMA) to obtain the SFMA, followed by preparing the SFMA hydrogel by ultraviolet (UV) crosslinking [32]. Then, the SFMA hydrogel was immersed in TA solution, and by varying the TA concentration and immersion time, the adhesion energy of the ST hydrogel was adjusted and optimized to ensure that the hydrogel had good tissue adhesion and separable abilities. Next, a PUA coating encapsulated the ST hydrogel to prepare a PUA-coated ST hydrogel with improved water retention capability. In addition, the swelling ratio, blood coagulation, *in vivo* hemostasis, and biocompatibility of the hydrogel were evaluated. Finally, by establishing a full-thickness model of rats, the effect of the PUA-coated ST hydrogel on promoting wound healing efficiency was examined.

RESULTS AND DISCUSSION

Adhesion properties of the hydrogel

Silk is a natural protein polymer that has been approved for medical use by the U.S. Food and Drug Administration (FDA) [33]. SF was processed from mulberry silk, which possesses excellent biocompatibility, controllable biodegradability, remarkable mechanical strength, and low immunogenicity [32,34,35]. Most importantly, the SF had remarkable mechanical strength and could induce the formation of thrombin to accelerate blood coagulation [17,35,36]. Therefore, SF has been widely used for wound healing [14,17,37]. After being modified by GMA, the UV-cross-linkable SFMA was synthesized (Fig. S1a). As shown in Fig. S1b, new peaks (in the region of 5.8–6.2 ppm) ascribed to C=C double bonds could be observed in the ^{1}H nuclear magnetic resonance (NMR) spectrum of SFMA, indicating the successful modification. With the presence of lithium phenyl-2,4,6-trimethylbenzoylphosphinate (LAP) as a photoinitiator, SFMA hydrogel was formed by exposing 15 wt% SFMA solution to UV light for 15 s. However, the SFMA

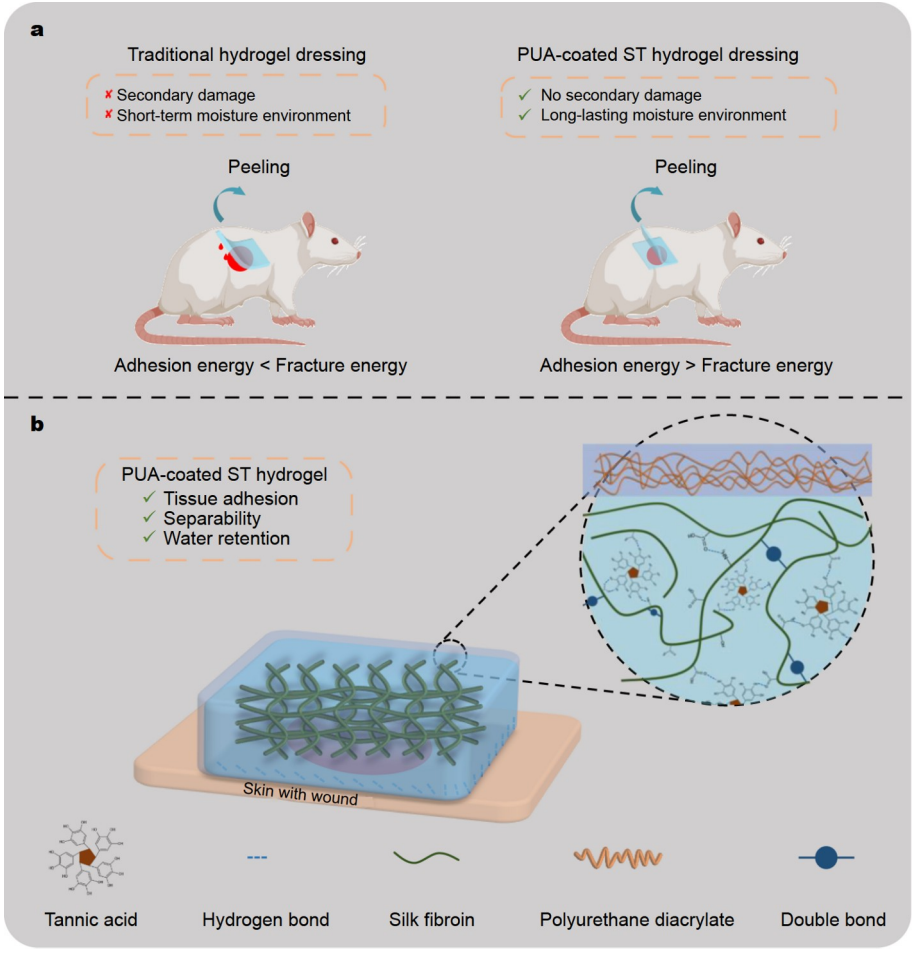

Figure 1 (a) Comparison of traditional hydrogel dressing and PUA-coated ST hydrogel dressing. (b) Schematic of the structure of the PUA-coated ST hydrogel.

hydrogel had almost no adhesion properties. TA, an FDA-approved polyphenol from nature involving abundant pyrogallol and catechol groups, allows strong adhesion between hydrogels and various materials through hydrogen bonding, π–π interaction, and metal chelation (Fig. 2a) [14,34,38]. By immersing SFMA hydrogel in TA solution, the ST hydrogel with adhesive properties could be obtained [17].

The 180-degree peel test was applied to quantify the adhesion energy of the SFMA/TA hydrogel. As shown in Fig. 2c, d, with the increasing concentration of TA and immersion time, the adhesion energy increased initially and then decreased. When the concentration of TA was 5 wt% and the immersion time was 2 h, the adhesion energy of the ST hydrogel reached a peak (52.6 ± 3.8 J m^{-2}). The ST hydrogel with peak adhesion energy was selected to do next experiments. Moreover, this ST hydrogel could tightly adhere to the fingers with different bending angles (0°, 45°, 90°, and 135°) and to other materials such as rubber, metal, glass, and plastic (Fig. 2b). Interestingly, this hydrogel adhered to fingers could be separated upon peeling and then leave a residual adhesive to the skin (Fig. 2e), possibly because the adhesion energy of this hydrogel was higher than its fracture energy [39]. The next fracture energy test showed that the fracture energy of the hydrogel was 32.7 ± 2.4 J m^{-2}, which was lower than its adhesion energy. Meanwhile, the inseparable control group was obtained by adding 10 wt% methacrylated polyethylene glycol (PEGMA) to the ST hydrogel to increase its mechanical properties [40]. Fig. S1c shows the ^{1}H NMR spectrum of PEGMA, and the degree of substitution of methacrylate groups in PEGMA was approximately 65.83%. Similar to ST hydrogel, after being immersed in 5 wt% TA solution for 2 h, the PEGMA/ST (PST) hydrogel could reach a peak of adhesion energy (55.9 ± 6.6 J m^{-2}), which was lower than its fracture energy (228.7 ± 44.5 J m^{-2}) (Fig. S2). Contrary to the ST hydrogel, the PST hydrogel was inseparable upon peeling (Fig. 2f). Based on the above data, this separable ST hydrogel might be suitable as wound dressing to reduce the damage to the wound during dressing changes.

Mechanical properties of the hydrogel

Not only increasing the adhesion energy, but also the addition of TA could enhance the mechanical strength of the ST hydrogel due to the hydrogen bonding interactions between SFMA chains and TA [14,17]. This interaction endowed the ST hydrogel with a smaller pore size than that of the SFMA hydrogel (Fig. S3). To

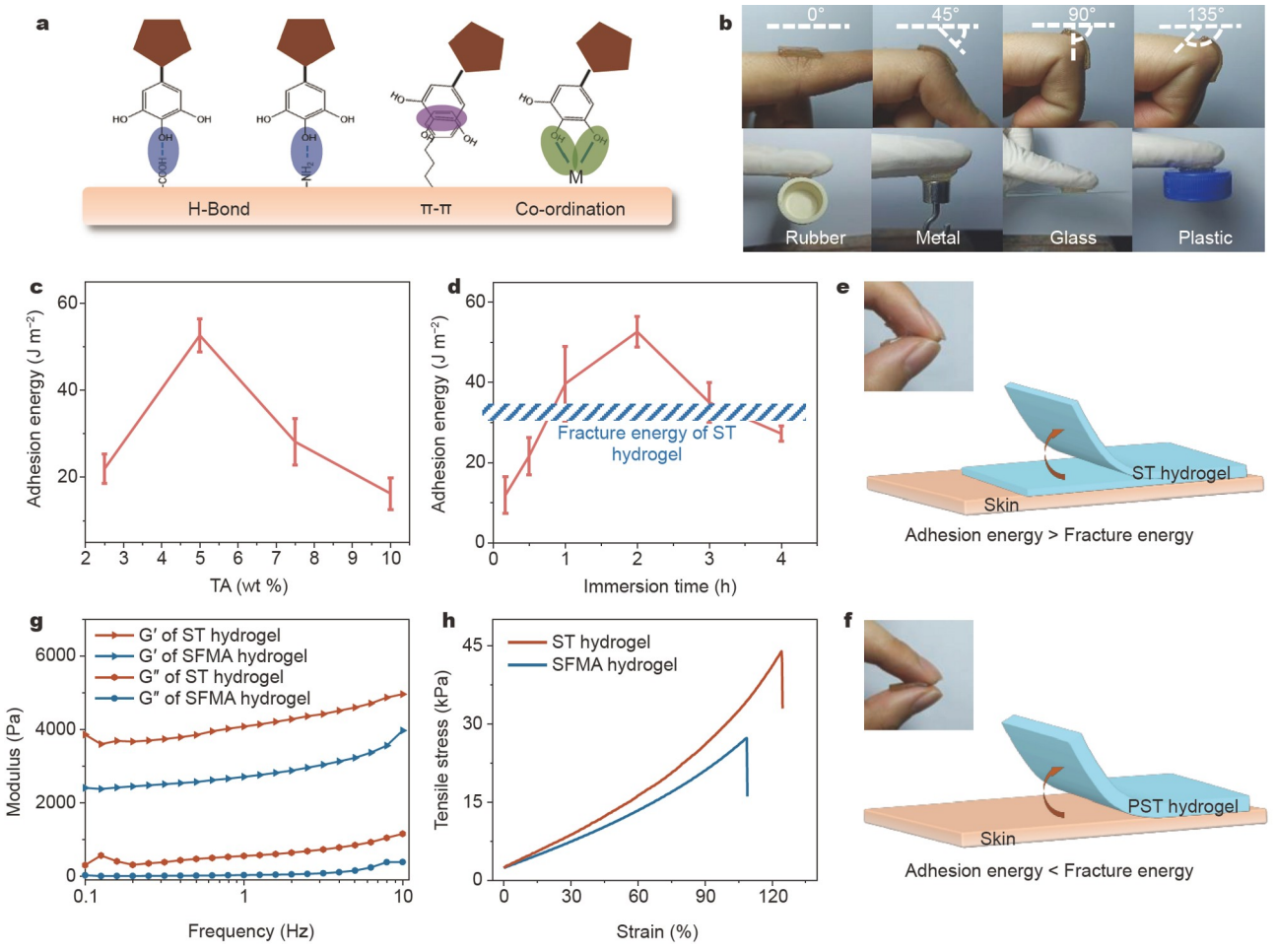

Figure 2 (a) Adhesion mechanism of the hydrogel treated by TA solution. (b) Photographs showed the ST hydrogels adhered to fingers with different bending angles (0°, 45°, 90°, and 135°) and to other materials (rubber, metal, glass, and plastic). (c) Adhesion energy of ST hydrogel with different concentrations of TA. (d) Adhesion energy of ST hydrogel with different immersion times. (e) Photo and scheme of the separable ST hydrogel upon peeling. (f) Photo and scheme of the inseparable PST hydrogel upon peeling. (g) Storage/loss (G', G'') modulus of SFMA and ST hydrogels. (h) Typical tensile stress-strain curves of SFMA and ST hydrogels.

determine the rheological properties of SFMA and ST hydrogels, a 1% strain frequency (0.1–10 Hz) sweep test was carried out to monitor the G' and G'' after the hydrogels were formed. As shown in Fig. 2g, the G' values were higher than the G'' in the whole frequency range, which indicated that the formed hydrogels exhibited a significantly elastic behavior. In addition, the G' values of the ST hydrogel were always higher than that of the SFMA hydrogel. Furthermore, the tensile tests (Fig. S4a) of the two hydrogels were also performed. Fig. 2h shows that the maximum tensile strengths of the SFMA and ST hydrogels were about 22.3 and 40.3 kPa, respectively. The rheological and tensile tests both demonstrated that TA could improve the mechanical strength of the ST hydrogel. Next, a fifty-cycle tensile test was carried out at a strain of 80% (Fig. S4b). A similar hysteresis curve was observed for all cycles, demonstrating that the ST hydrogel had good fatigue resistance.

Formation and functions of PUA coating

Fig. 3a schematically shows the formation of the PUA coating on the surfaces of the ST hydrogel. In the first step, the cylinder-shaped ST hydrogel (diameter = 15 mm, thickness = 2 mm) was placed in a bath, and then immersed in the 0.5 wt% I2959 (a water/oil soluble photoinitiator) solution for 5 min. The hydrogel was taken out and the residual I2959 solution on the surface was wiped off. As shown in Fig. S5, through the reversion procedure, the hydrogel could obtain better water-retention capability, so, in the second step, the hydrogel was reversed and suspended in the oligomeric UDA bath. By exposing the bottom of the UDA bath to the UV light (365 nm), the free-radical polymerization of the UDA oligomer would be triggered by the I2959 photoinitiator to form the PUA coating. Finally, except for the surface 2, the hydrogel was encapsulated by a transparent and shape-fitted PUA coating.

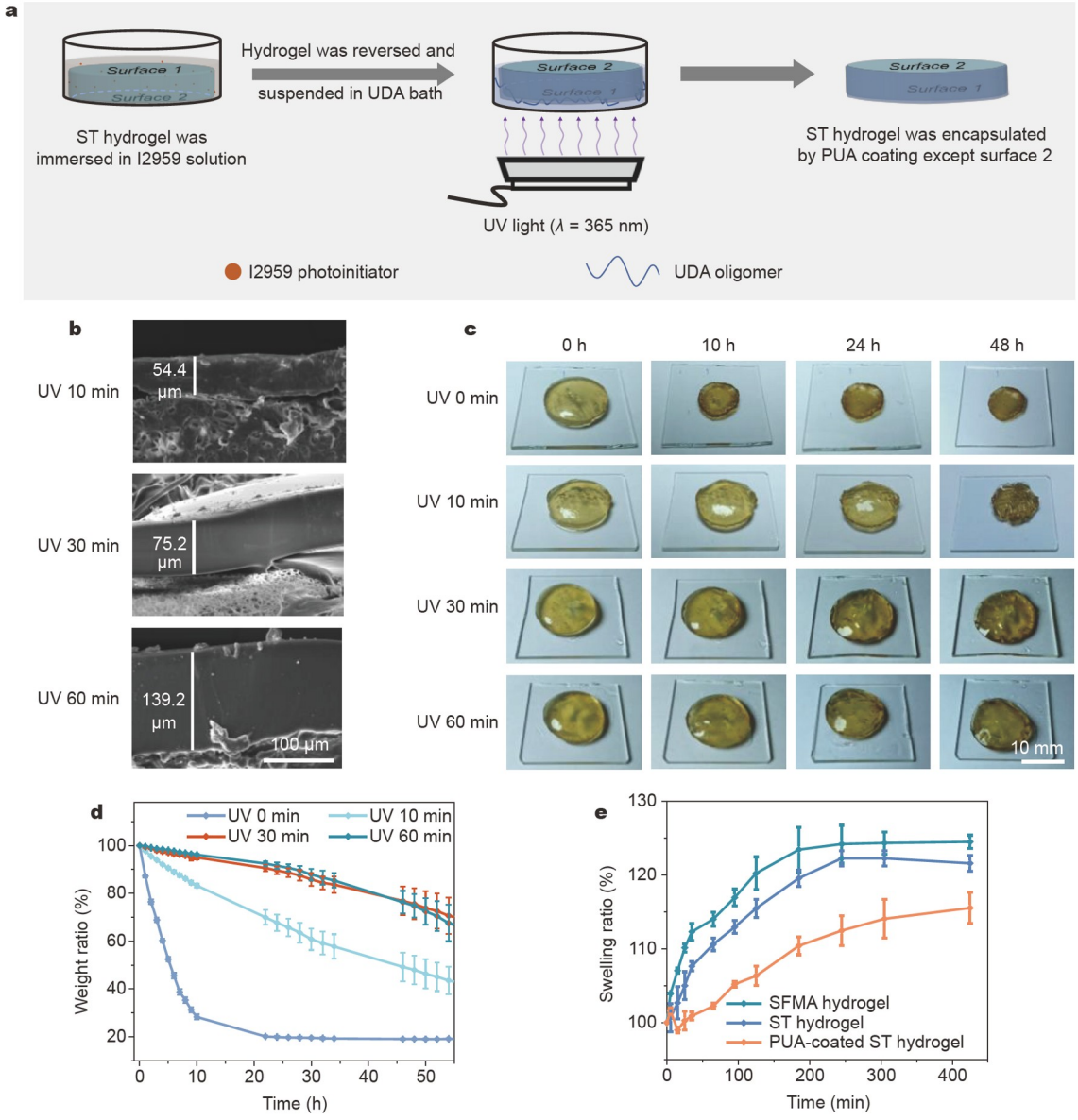

Figure 3 Formation and functions of PUA coating. (a) Schematic diagram of the PUA coating fabrication around ST hydrogel except for the surface 2. (b) SEM images of coatings formed by different UV exposure times (10, 30, and 60 min). (c) Photos at given times (0, 10, 24, and 48 h) of hydrogels with varying thicknesses of coatings formed by different UV exposure times (0, 10, 30, and 60 min). (d) Weight ratio of hydrogels with time. (e) Swelling ratio of hydrogels with time.

Scanning electron microscopy (SEM) images (Fig. 3b) indicated that by extending the polymerization time from 10 to 60 min, the thickness of PUA coating increased from about 54.4 to 139.2 μm. Next, the water retention capability of hydrogels with varying thicknesses of coatings was tested (Fig. 3c, d). The hydrogel without coating noticeably shrank, and the weight ratio of it was only 28.3 ± 1.1 wt% at 10 h due to the quick water evaporation, and then reached equilibrium (19.9 ± 0.4 wt%) at about 24 h. In comparison, the water retention capability of hydrogels with coatings significantly increased. When the polymerization time of PUA coating was 10 min, the hydrogel could maintain its shape till 24 h, but it would shrink obviously at 48 h, and the weight ratio was only 48.0 ± 6.0 wt%. When the polymerization time was prolonged to 30 and 60 min, the size of corresponding hydrogels showed almost no change at 48 h. Besides, there was no noticeable difference between the weight ratios of the two hydrogels. Based on the water retention capability and polymerization efficiency, we selected the 30 min polymerization time for all subsequent studies, and the ST hydrogel encapsulated by the coating was named PUA-coated ST hydrogel. The low swelling ratio property was also essential to hydrogel dressings because it could decrease the weak mechanical toughness caused by absorbing wound exudate [41,42]. As shown in Fig. 3e, due to the interactions between SFMA chains and TA molecules, the ST hydrogel had a lower swelling ratio than the SFMA hydrogel. The existence of PUA coating could further decrease the swelling ratio by encapsulating the ST hydrogel. In summary, because of the good water retention capability and low swelling ratio, the PUA-coated ST hydrogel could be a hydrogel dressing for wound healing.

Hemostasis properties of the hydrogel

Generally, hydrogel's good tissue adhesive property will give it good hemostatic properties [43]. The *in vitro* hemostatic property of the hydrogel was evaluated by the blood coagulation index (BCI), where the higher BCI value showed a lower clotting rate. Fig. 4a shows the control and gauze groups had higher BCI values than the hydrogel group. Next, the tail amputation model of mice was further established to evaluate the *in vivo* hemostatic property of the hydrogel (Fig. 4b). As shown in Fig. 4c, the blood loss from the control group (135.0 ± 9.5 mg) was the highest. After being treated with gauze and hydrogel, the blood loss reduced to 78.7 ± 18.7 and 41.3 ± 5.0 mg. Fig. 4d shows that the hemostasis time of the adhesive hydrogel group (126.7 ± 21.4 s) was distinctly shorter than that of the blank (254.3 ± 18.4 s) and gauze (163.3 ± 6.5 s) groups. Gauze had hemostasis properties by absorbing blood plasma to concentrate red blood cells (RBCs) and coagulation factors [44,45]. On the one hand, the hydrogel could stick to the blood area and act as a physical barrier to prevent blood loss. On the other hand, the hydrogen bonding interactions between TA and proteins in blood might also decrease bleeding [16]. Furthermore, SF could induce the formation of thrombin to accelerate blood coagulation [36]. Based on the above data, this adhesive hydrogel had good hemostatic properties.

Biocompatibility of the hydrogel

Good biocompatibility was a precondition for wound-healing biomaterials. The rupture of RBCs would lead to the release of platelet, hemoglobin, and even thrombus formation, so the RBCs compatibility was of great importance to wound dressing in contact with blood [46]. A hemolytic activity assay was used to evaluate the hemolysis ratio of the hydrogel. Fig. 5a shows that the hemolysis ratio of the hydrogel was considerably lower than that of the ddH_2O group. Besides, the cytocompatibility test of the hydrogel with L929 cells was evaluated. As shown in Fig. 5b, the optical density at 450 nm (OD_{450}) indicated that over 85% of cells of the hydrogel group remained survival at 12, 24, and 48 h, which was much higher than the lowest acceptable standard of nontoxicity of biomaterials (70%) [47,48]. The confocal images

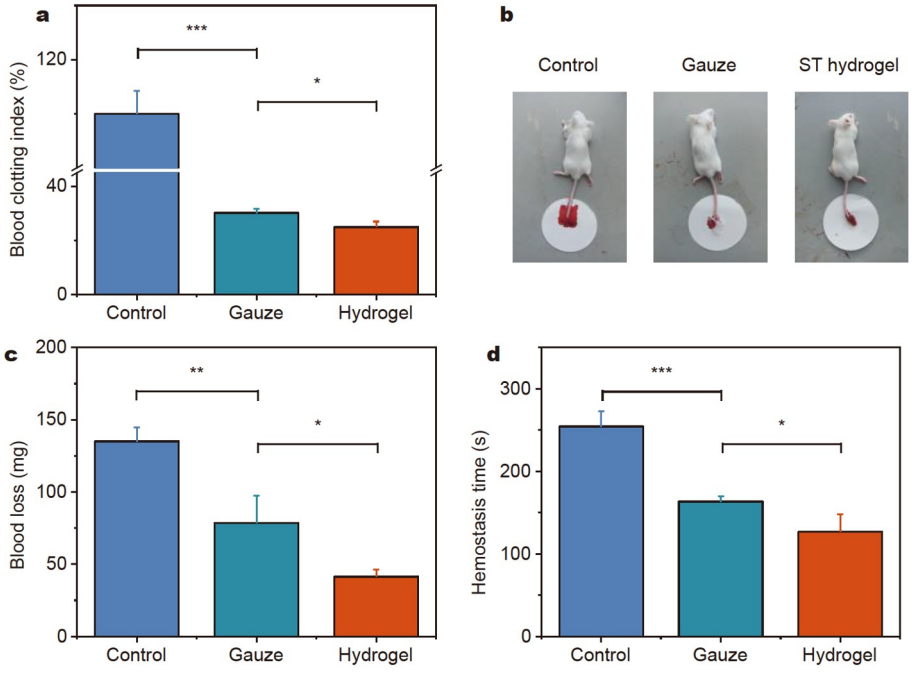

Figure 4 Hemostasis properties of the hydrogel. (a) Blood clotting indexes in the control group, gauze group, and hydrogel group. (b) Pictures of blood collected during hemostasis among different groups. (c) Blood losses and (d) hemostasis times for different groups.

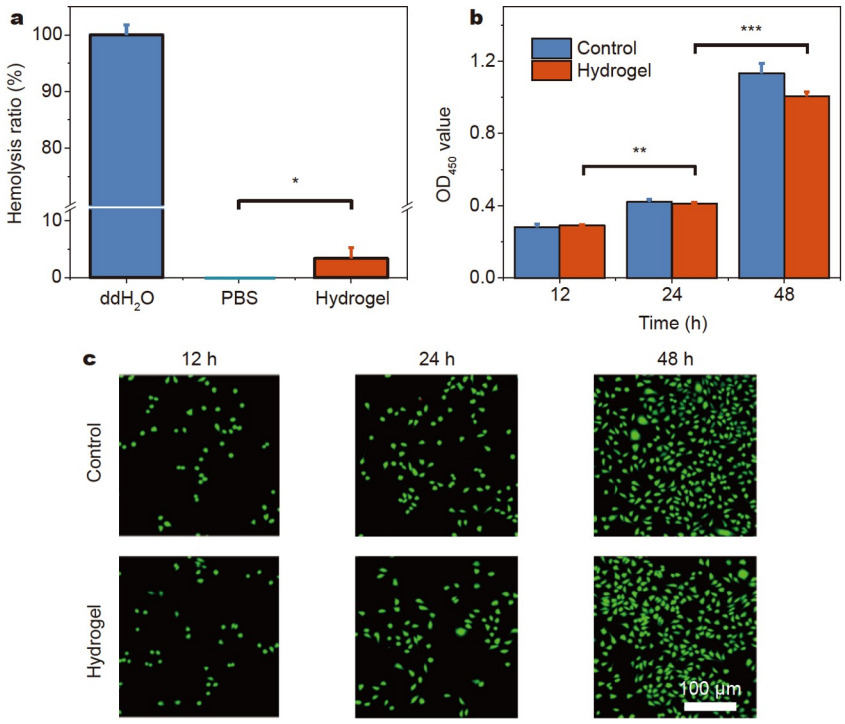

Figure 5 Biocompatibility properties of hydrogel. (a) Hemolysis ratios for different groups. (b) OD_{450} values and (c) Live/dead staining pictures of control and hydrogel groups at 12, 24, and 48 h.

of live/dead cell staining (Fig. 5c) indicated that the density of live cells (green fluorescence) of the control and hydrogel groups continuously increased with culturing, and almost no dead cells (red fluorescence) were found. Overall, these hemocompatibility and cytocompatibility results suggest the good biocompatibility of the hydrogel.

Acceleration of PUA-coated ST hydrogel for wound healing

Before the animal experiments, the thickness of the residual adhesive after ten dressing changes was tested. Fig. S6 shows that the thicknesses of the residual adhesives with no patch change and ten patch changes were almost the same. This indicated that the residual adhesive contact on the skin would not be thicker with dressing changes. To assess the practical therapeutic effect of the PUA-coated ST hydrogel, *in vivo* full-thickness skin defects (diameter = 10 mm) were created on the back of SD rats. These rats were randomly divided into five groups: blank, gauze, ST hydrogel, PUA-coated PST hydrogel, and PUA-coated ST hydrogel groups. The wound healing processes of the five groups were recorded on days 0, 3, 6, and 12 with a digital camera (Fig. 6a). To further visually illustrate the difference in wound healing efficiency between these groups, their dynamic healing processes are shown in Fig. 6c. It was clear that three hydrogel groups had higher healing efficiency than the blank and gauze groups mainly because of the moist environment provided by the hydrogels [15,49]. It could also be seen in Fig. 6b, the wound closure rate of the PUA-coated ST hydrogel group on day 12 was 96.9% ± 0.6%, which was higher than that of the PUA-coated PST hydrogel group (92.2% ± 0.6%), ST hydrogel group (89.1% ± 0.7%), gauze group (82.4% ± 1.2%), and the blank group (86.4% ± 1.2%).

The wound healing efficiency of the gauze group was the lowest because the gauze easily adhered to the wound after absorbing the wound exudate, leading to severe secondary damage to the wound during removal [7,50]. Although ST hydrogel had the advantage of a moist environment in wound healing, this advantage would quickly disappear because ST hydrogel dehydrated rapidly. Owing to the adhesion energy being lower than the fracture energy, the PUA-coated PST hydrogel dressing was inseparable, which would cause damage to the wound during dressing changes. In particular, the PUA-coated ST hydrogel group achieved the highest wound healing efficiency among the three hydrogel groups. On the one hand, the PUA coating endowed the PUA-coated ST hydrogel dressing with a long-lasting water retention capability, allowing for more efficient wound healing by providing a long-lasting moist healing environment. On the other hand, because the adhesion energy was higher than the fracture energy, the PUA-coated ST hydrogel was separable, and residual hydrogel still adhered to the wound, so there was almost no damage to the wound during dressing changes. In conclusion, the wound healing efficiency of the PUA-coated ST hydrogel group was the highest among the five groups.

The quality of the wound healing in the five groups on day 12 was further evaluated by hematoxylin and eosin (H&E) and Masson staining (Fig. 7a). The shorter the wound width, the better tissue healing [7]. Fig. 7b demonstrates that the wound width of the PUA-coated ST hydrogel group (0.558 ± 0.021 mm) was the shortest among all groups, and the figures for the PUA-coated PST hydrogel group, ST hydrogel group, gauze group, and blank group were 1.375 ± 0.239, 1.940 ± 0.164, 2.940 ± 0.453, and 2.126 ± 0.155 mm, respectively. Furthermore, the higher the collagen index, the better collagen deposition in the wound [47]. The collagen index results (Fig. 7c) showed that the hydrogel groups, especially the PUA-coated ST hydrogel group (66.5% ± 6.0%), significantly enhanced the deposition of col-

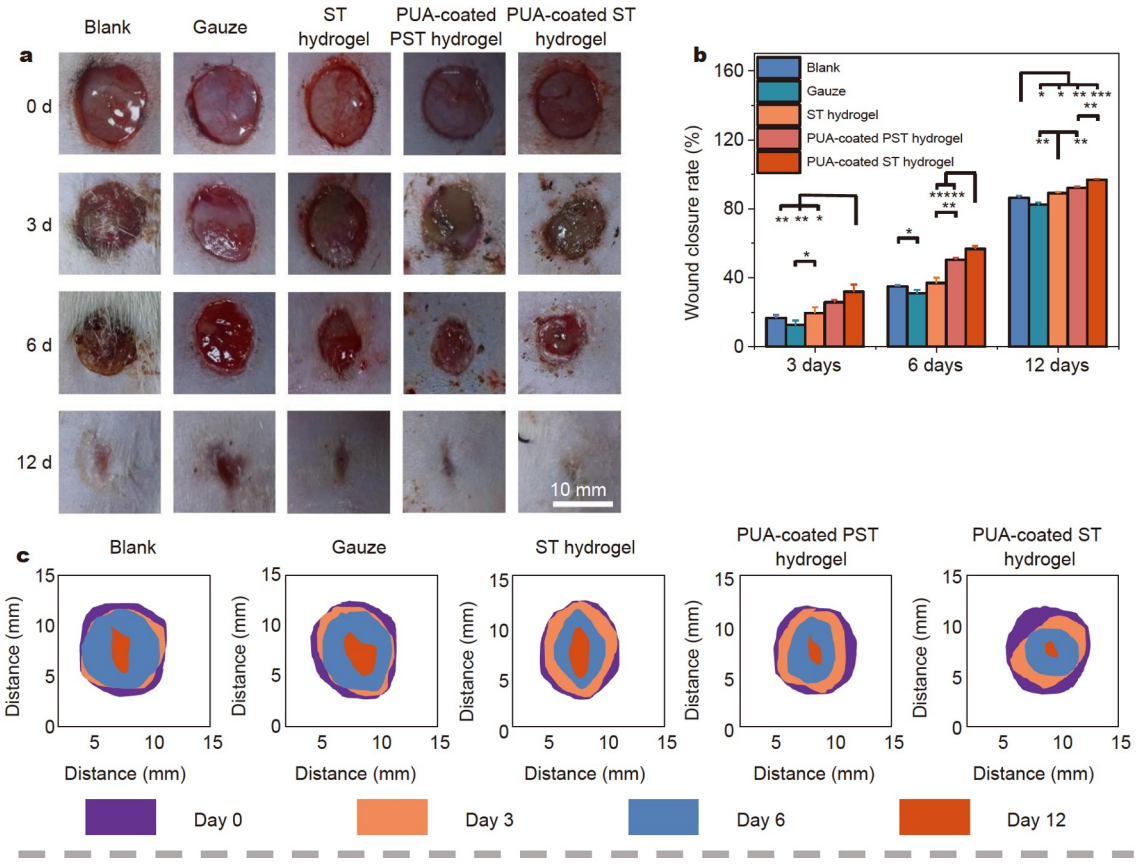

Figure 6 (a) Photos of wound at days 3, 6, and 12. (b) Wound closure rates of the five groups at days 3, 6, and 12. (c) Wound trace of the five groups.

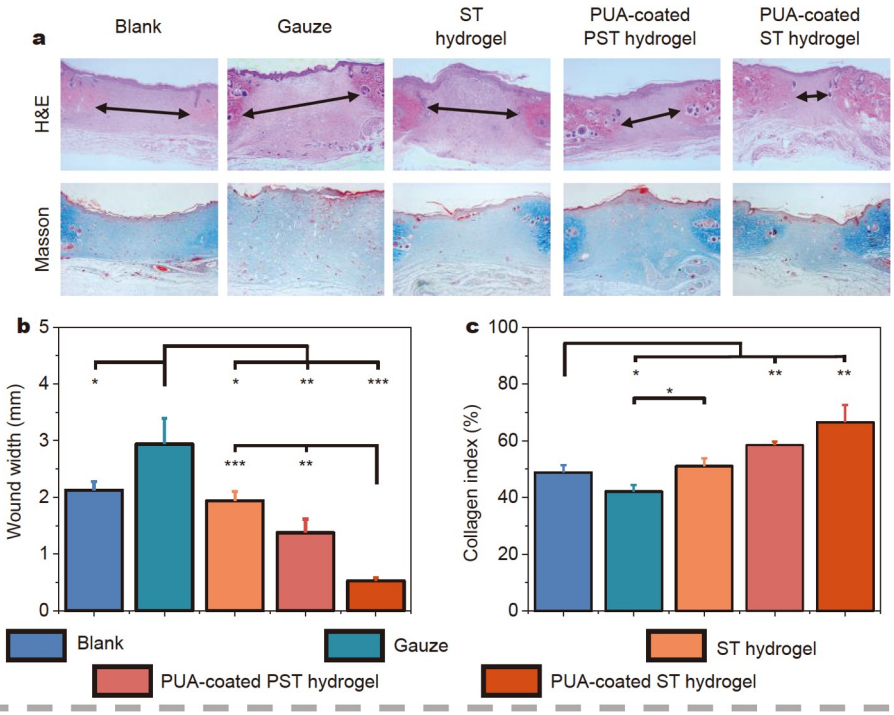

Figure 7 (a) H&E and Masson staining results on day 12. Black two-way arrows indicate the wound width. Blue color represents collagen deposition. (b) Wound width and (c) collagen index on day 12.

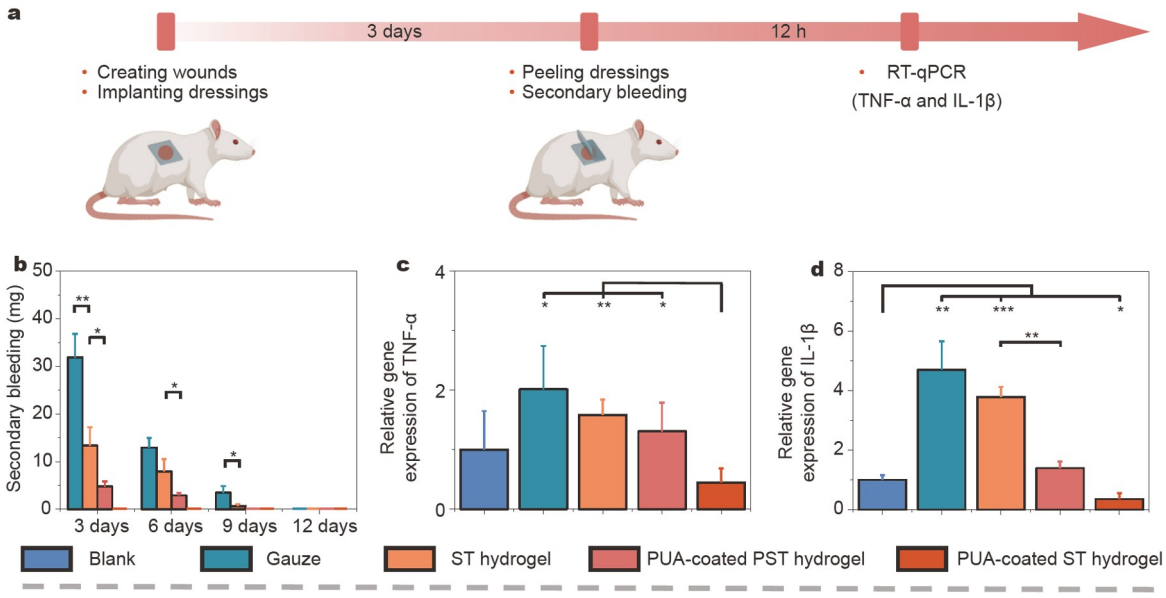

Figure 8 Evaluation of secondary damage. (a) Workflow for evaluating secondary damage and the schematic diagram of dressings being implanted in the wound defects. (b) Secondary bleeding when changing different dressings. Relative gene expressions of (c) TNF-α and (d) IL-1β at 12 h after the first changing dressings.

lagen compared with the PUA-coated PST hydrogel (58.5% ± 1.2%), ST hydrogel (51.0% ± 2.7%), gauze (42.2 ± 2.4%), and blank (48.8% ± 2.6%) groups. These histological data agreed well with the observation on wound healing.

The evaluation of secondary damage

The secondary damage of the five groups was further evaluated to reveal the mechanism of PUA-coated ST hydrogel for accelerating wound healing (Fig. 8a). Because of the re-damage to the wound, secondary damage during dressing changes could be seen as a new injury to the wound and result in secondary bleeding and increased relative gene expression of inflammation factors [22]. Fig. 8b shows that the secondary bleeding of the PUA-coated ST hydrogel group was the lowest at any changing dressings. In addition, the related inflammation factors (TNF-α and IL-1β) markedly increased at about 12 h after a new injury [13,51,52]. Therefore, the relative gene expression of TNF-α and IL-1β at 12 h after the first changing dressings was tested by real time quantitative polymerase chain reaction (RT-qPCR). The primer sequences for RT-qPCR are listed in Table S1. The results (Fig. 8c, d) indicated that the PUA-coated ST hydrogel group had the lowest relative gene expression of the two inflammation factors. These results were most likely due to the long-lasting water retention and separable abilities of the PUA-coated ST hydrogel.

CONCLUSIONS

In this study, we developed a water-retaining and separable adhesive PUA-coated ST hydrogel wound dressing with good hemostatic properties and biocompatibility. The evaluation of adhesion energy and fracture energy showed that the separable ST hydrogel could be obtained by immersing the SFMA hydrogel in 5 wt% TA solution for 2 h. Next, the hydrophobic PUA coating was formed on the surfaces of the hydrogel to prevent water evaporation. Compared with the blank, gauze, ST hydrogel, and PUA-coated PST hydrogel dressings, the PUA-coated ST hydrogel dressing could improve the wound healing efficiency by not only providing a long-lasting moist environment but also being separated without secondary damage during dressing changes. Besides, it should be noted that the residual adhesive could not be removed, so for wounds that need cleaning, such as infected wounds, this hydrogel dressing might be not suitable. In summary, the PUA-coated ST hydrogel promoted wound healing and brought a new strategy for the next-generation design of adhesive hydrogel wound dressings.

Received 24 December 2022; accepted 31 March 2023; published online 14 June 2023

1 Li Z, Zhou F, Li Z, *et al.* Hydrogel cross-linked with dynamic covalent bonding and micellization for promoting burn wound healing. ACS Appl Mater Interfaces, 2018, 10: 25194–25202
2 Dimatteo R, Darling NJ, Segura T. *In situ* forming injectable hydrogels for drug delivery and wound repair. Adv Drug Deliver Rev, 2018, 127: 167–184
3 Hao R, Cui Z, Zhang X, *et al.* Rational design and preparation of functional hydrogels for skin wound healing. Front Chem, 2021, 9: 839055
4 Zhao X, Liang Y, Huang Y, *et al.* Physical double-network hydrogel adhesives with rapid shape adaptability, fast self-healing, antioxidant and NIR/pH stimulus-responsiveness for multidrug-resistant bacterial infection and removable wound dressing. Adv Funct Mater, 2020, 30: 1910748
5 Dai Z, Zhang Y, Chen C, *et al.* An antifouling and antimicrobial zwitterionic nanocomposite hydrogel dressing for enhanced wound healing. ACS Biomater Sci Eng, 2021, 7: 1621–1630
6 Frykberg RG, Banks J. Challenges in the treatment of chronic wounds. Adv Wound Care, 2015, 4: 560–582
7 Huangfu Y, Li S, Deng L, *et al.* Skin-adaptable, long-lasting moisture, and temperature-tolerant hydrogel dressings for accelerating burn wound healing without secondary damage. ACS Appl Mater Interfaces, 2021, 13: 59695–59707
8 Li S, Chen A, Chen Y, *et al.* Lotus leaf inspired antiadhesive and antibacterial gauze for enhanced infected dermal wound regeneration. Chem Eng J, 2020, 402: 126202

9 Junker JPE, Kamel RA, Caterson EJ, *et al.* Clinical impact upon wound healing and inflammation in moist, wet, and dry environments. Adv Wound Care, 2013, 2: 348–356
10 Dyson M, Young SR, Hart J, *et al.* Comparison of the effects of moist and dry conditions on the process of angiogenesis during dermal repair. J Investig Dermatol, 1992, 99: 729–733
11 Winter GD. Formation of the scab and the rate of epithelization of superficial wounds in the skin of the young domestic pig. Nature, 1962, 193: 293–294
12 Zhang L, Liu M, Zhang Y, *et al.* Recent progress of highly adhesive hydrogels as wound dressings. Biomacromolecules, 2020, 21: 3966–3983
13 Liang Y, He J, Guo B. Functional hydrogels as wound dressing to enhance wound healing. ACS Nano, 2021, 15: 12687–12722
14 Pan G, Li F, He S, *et al.* Mussel- and barnacle cement proteins-inspired dual-bionic bioadhesive with repeatable wet-tissue adhesion, multimodal self-healing, and antibacterial capability for nonpressing hemostasis and promoted wound healing. Adv Funct Mater, 2022, 32: 2200908
15 Cao C, Yang N, Zhao Y, *et al.* Biodegradable hydrogel with thermoresponse and hemostatic effect for photothermal enhanced anti-infective therapy. Nano Today, 2021, 39: 101165
16 Xu G, Xu N, Ren T, *et al.* Multifunctional chitosan/silver/tannic acid cryogels for hemostasis and wound healing. Int J Biol Macromolecules, 2022, 208: 760–771
17 He X, Liu X, Yang J, *et al.* Tannic acid-reinforced methacrylated chitosan/methacrylated silk fibroin hydrogels with multifunctionality for accelerating wound healing. Carbohydrate Polyms, 2020, 247: 116689
18 Fan H, Wang J, Zhang Q, *et al.* Tannic acid-based multifunctional hydrogels with facile adjustable adhesion and cohesion contributed by polyphenol supramolecular chemistry. ACS Omega, 2017, 2: 6668–6676
19 Wang B, Xin T, Shen L, *et al.* Acoustic transmitted electrospun fibrous membranes for tympanic membrane regeneration. Chem Eng J, 2021, 419: 129536
20 Liu H, Qin S, Liu J, *et al.* Bio-inspired self-hydrophobized sericin adhesive with tough underwater adhesion enables wound healing and fluid leakage sealing. Adv Funct Mater, 2022, 32: 2201108
21 Liu B, Wang Y, Miao Y, *et al.* Hydrogen bonds autonomously powered gelatin methacrylate hydrogels with super-elasticity, self-heal and underwater self-adhesion for sutureless skin and stomach surgery and E-skin. Biomaterials, 2018, 171: 83–96
22 Guo B, Dong R, Liang Y, *et al.* Haemostatic materials for wound healing applications. Nat Rev Chem, 2021, 5: 773–791
23 Zhou Z, Xiao J, Guan S, *et al.* A hydrogen-bonded antibacterial curdlan-tannic acid hydrogel with an antioxidant and hemostatic function for wound healing. Carbohydr Polym, 2022, 285: 119235
24 Sekine Y, Ikeda-Fukazawa T. Structural changes of water in a hydrogel during dehydration. J Chem Phys, 2009, 130: 034501
25 Wu J, Wu Z, Xu H, *et al.* An intrinsically stretchable humidity sensor based on anti-drying, self-healing and transparent organohydrogels. Mater Horiz, 2019, 6: 595–603
26 Ying B, Liu X. Skin-like hydrogel devices for wearable sensing, soft robotics and beyond. iScience, 2021, 24: 103174
27 Subraveti SN, Raghavan SR. A simple way to synthesize a protective "skin" around any hydrogel. ACS Appl Mater Interfaces, 2021, 13: 37645–37654
28 Zhu T, Jiang C, Wang M, *et al.* Skin-inspired double-hydrophobic-coating encapsulated hydrogels with enhanced water retention capacity. Adv Funct Mater, 2021, 31: 2102433
29 Mredha MTI, Le HH, Cui J, *et al.* Double-hydrophobic-coating through quenching for hydrogels with strong resistance to both drying and swelling. Adv Sci, 2020, 7: 1903145÷÷
30 Jiang Y, Zhang X, Zhang W, *et al.* Infant skin friendly adhesive hydrogel patch activated at body temperature for bioelectronics securing and diabetic wound healing. ACS Nano, 2022, 16: 8662–8676
31 Liang Y, Li Z, Huang Y, *et al.* Dual-dynamic-bond cross-linked antibacterial adhesive hydrogel sealants with on-demand removability for post-wound-closure and infected wound healing. ACS Nano, 2021, 15: 7078–7093
32 Kim SH, Hong H, Ajiteru O, *et al.* 3D bioprinted silk fibroin hydrogels for tissue engineering. Nat Protoc, 2021, 16: 5484–5532
33 Zhang W, Chen L, Chen J, *et al.* Silk fibroin biomaterial shows safe and effective wound healing in animal models and a randomized controlled clinical trial. Adv Healthcare Mater, 2017, 6: 1700121
34 Bai S, Zhang X, Cai P, *et al.* A silk-based sealant with tough adhesion for instant hemostasis of bleeding tissues. Nanoscale Horiz, 2019, 4: 1333–1341
35 Kundu B, Rajkhowa R, Kundu SC, *et al.* Silk fibroin biomaterials for tissue regenerations. Adv Drug Deliver Rev, 2013, 65: 457–470
36 Seib FP, Maitz MF, Hu X, *et al.* Impact of processing parameters on the haemocompatibility of Bombyx mori silk films. Biomaterials, 2012, 33: 1017–1023
37 Guan G, Zhang Q, Jiang Z, *et al.* Multifunctional silk fibroin methacryloyl microneedle for diabetic wound healing. Small, 2022, 18: 2203064
38 Zhang Q, Qiao Y, Li C, *et al.* Chitosan/gelatin-tannic acid decorated porous tape suture with multifunctionality for tendon healing. Carbohydrate Polyms, 2021, 268: 118246
39 Yang C, Suo Z. Hydrogel ionotronics. Nat Rev Mater, 2018, 3: 125–142
40 Zhang X, Chen G, Wang Y, *et al.* Arrowhead composite microneedle patches with anisotropic surface adhesion for preventing intrauterine adhesions. Adv Sci, 2022, 9: 2104883
41 Xu Q, A S, Gao Y, *et al.* A hybrid injectable hydrogel from hyperbranched PEG macromer as a stem cell delivery and retention platform for diabetic wound healing. Acta Biomater, 2018, 75: 63–74
42 Zhang L, Zhang Y, Ma F, *et al.* A low-swelling and toughened adhesive hydrogel with anti-microbial and hemostatic capacities for wound healing. J Mater Chem B, 2022, 10: 915–926
43 Liang Y, Li M, Yang Y, *et al.* pH/glucose dual responsive metformin release hydrogel dressings with adhesion and self-healing *via* dual-dynamic bonding for athletic diabetic foot wound healing. ACS Nano, 2022, 16: 3194–3207
44 Zhang W, Wu J, Yu L, *et al.* Paraffin-coated hydrophobic hemostatic zeolite gauze for rapid coagulation with minimal adhesion. ACS Appl Mater Interfaces, 2021, 13: 52174–52180
45 Xu Y, Fang Y, Ou Y, *et al.* Zinc metal-organic framework@chitin composite sponge for rapid hemostasis and antibacterial infection. ACS Sustain Chem Eng, 2020, 8: 18915–18925
46 Song X, Wang K, Tang CQ, *et al.* Design of carrageenan-based heparin-mimetic gel beads as self-anticoagulant hemoperfusion adsorbents. Biomacromolecules, 2018, 19: 1966–1978
47 Qian J, Ji L, Xu W, *et al.* Copper-hydrazide coordinated multifunctional hyaluronan hydrogels for infected wound healing. ACS Appl Mater Interfaces, 2022, 14: 16018–16031
48 Bahadoran M, Shamloo A, Nokoorani YD. Development of a polyvinyl alcohol/sodium alginate hydrogel-based scaffold incorporating bFGF-encapsulated microspheres for accelerated wound healing. Sci Rep, 2020, 10: 7342
49 Yu R, Zhang H, Guo B. Conductive biomaterials as bioactive wound dressing for wound healing and skin tissue engineering. Nano-Micro Lett, 2022, 14: 1
50 Zhang M, Zhao X. Alginate hydrogel dressings for advanced wound management. Int J Biol Macromol, 2020, 162: 1414–1428
51 Hübner G, Brauchle M, Smola H, *et al.* Differential regulation of pro-inflammatory cytokines during wound healing in normal and glucocorticoid-treated mice. Cytokine, 1996, 8: 548–556
52 Sato Y, Ohshima T. The expression of mRNA of proinflammatory cytokines during skin wound healing in mice: A preliminary study for forensic wound age estimation (II). Int J Legal Med, 2000, 113: 140–145

Acknowledgements This work was supported by the National Natural Science Foundation of China (31971326 and 52203205).

Author contributions Zhang Z performed the experiments and wrote the original manuscript. Zhang Y and Wang J supervised the experiments and revised the manuscript. Liu Y and Liu X guided the synthesis of hydrogel.

Zheng P and Gao T participated in the mechanical tests. Luo B and Ma F carried out the cell experiments. Pei R guided the work. All authors have given approval to the final version of the manuscript.

Conflict of interest The authors declare that they have no conflict of interest.

Supplementary information Experimental details and supporting data are available in the online version of this paper.

Zhuangzhuang Zhang is studying for his Master's degree at the School of Nano-Tech and Nano-Bionics, University of Science and Technology of China (USTC). His current research focuses on the synthesis of adhesive hydrogels for wound healing applications.

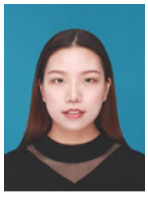

Yajie Zhang received her PhD degree from the USTC in 2020. Currently, she is working as a postdoctoral fellow at Suzhou Institute of Nano-Tech and Nano-Bionics, Chinese Academy of Sciences (CAS). Her research focuses on the synthesis and functionalization of biomaterials, and the synthesis of fast-crosslinking hydrogels as bio-scaffolds and 3D bioprinting for tissue regeneration.

Jine Wang received her PhD degree from Changchun Institute of Applied Chemistry, CAS in 2012. Now she is working at Suzhou Institute of Nano-Tech and Nano-Bionics, CAS as an associate professor. Her research includes aptamer-SELEX, synthesis of functional MOFs and applications in biomedicine, and implantable neural interface based on hydrogel.

Renjun Pei received his PhD degree from Wuhan University, and is currently working as a professor at the CAS Key Laboratory of Nano-Bio Interface, Suzhou Institute of Nano-Tech and Nano-Bionics, CAS. His current research interests include: (1) biomaterials, injectable hydrogels, and 3D bioprinting for tissue regeneration and (2) aptamer SELEX and applications, including light-up probes, *in vivo* MRI probes, isolation of circulating tumor cells, and targeted delivery nano-platforms.

用于伤口修复的无二次损伤的保水可撕断粘附水凝胶

张壮壮[1,2], 张雅洁[2*], 刘远山[1,2], 郑鹏辉[2], 高童[2], 罗冰清[1,2], 柳星竹[2], 马凡舒[2], 王金娥[1,2*], 裴仁军[1,2*]

摘要 作为新型伤口敷料, 粘附性水凝胶已被广泛研究. 然而, 由于易失水和敷料更换时二次损伤的问题, 粘附水凝胶敷料的临床应用仍然是一个重大挑战. 本文中, 我们设计了一种基于双键化丝素蛋白、单宁酸和聚氨酯二丙烯酸酯的具有保水性能和可撕断性能的粘附水凝胶敷料. 通过复合具有大量儿茶酚基团的单宁酸, 使得水凝胶具有增强的机械性能、良好的组织粘附性能、止血性能以及生物相容性能. 随后将疏水性的聚氨酯二丙烯酸酯涂层聚合在水凝胶表面, 该涂层的存在可以使水凝胶长时间保持高含水量. 此外, 由于该水凝胶的粘附能高于断裂能, 其在剥离时可以被撕断, 并最大程度减小对伤口部位的影响. 动物实验结果表明, 这种具有粘附止血性能的水凝胶可以通过提供长久的湿性愈合环境和无二次损伤的换料来加速伤口愈合. 这些结果表明这种多功能水凝胶是一种具有临床应用前景的伤口敷料.

